Colloids and Surfaces B: Biointerfaces 192 (2020) 111015

Contents lists available at ScienceDirect

Colloids and Surfaces B: Biointerfaces

journal homepage: www.elsevier.com/locate/colsurfb

Behavior of plant-dairy protein blends at air-water and oil-water interfaces

Emma B.A. Hinderink[a,b,*], Leonard Sagis[c], Karin Schroën[b], Claire C. Berton-Carabin[b]

[a] TiFN, P.O. Box 557, 6700 AN, Wageningen, the Netherlands
[b] Laboratory of Food Process Engineering, Bornse Weilanden 9, 6708 WG Wageningen, the Netherlands
[c] Laboratory of Physics and Physical Chemistry of Foods, Bornse Weilanden 9, 6708 WG Wageningen, the Netherlands

ARTICLE INFO

Keywords:
Interfacial rheology
Lissajous plot
Interface characterization
Plant protein
Dairy protein
Protein mixtures

ABSTRACT

Recent work suggests that using blends of dairy and plant proteins could be a promising way to mitigate sustainability and functionality concerns. Many proteins form viscoelastic layers at fluid interfaces and provide physical stabilization to emulsion droplets; yet, the interfacial behavior of animal-plant protein blends is greatly underexplored. In the present work, we considered pea protein isolate (PPI) as a model legume protein, which was blended with well-studied dairy proteins (whey protein isolate (WPI) or sodium caseinate (SC)). We performed dilatational rheology at the air-water and oil-water interface using an automated drop tensiometer to chart the behavior and structure of the interfacial films, and to highlight differences between films made with either blends, or their constituting components only.

The rheological response of the blend-stabilized interfaces deviated from what could be expected from averaging those of the individual proteins and depended on the proteins used; e.g. at the air-water interface, the response of the caseinate-pea protein blend was similar to that of PPI only. At the oil-water interface, the PPI and WPI-PPI interfaces gave comparable responses upon deformation and formed less elastic layers compared to the WPI-stabilized interface. Blending SC with PPI gave stronger interfacial layers compared to SC alone, but the layers were less stiff compared to the layers formed with WPI, PPI and WPI-PPI. In general, higher elastic moduli and more rigid interfacial layers were formed at the air-water interface, compared to the oil-water interface, except for PPI.

1. Introduction

Many food products are multiphase systems, such as foams and emulsions. These products often contain proteins, which are amphiphilic molecules that adsorb at the air-water or oil-water interface, and thereby play a crucial role in the formation and stability of the systems. Protein adsorption reduces the surface free energy, which facilitates small bubble and droplet formation during homogenization; and next, proteins form an interfacial layer that protects bubbles and droplets against physical destabilization, either by inducing steric/electrostatic repulsion, or by forming viscoelastic layers that mechanically prevent coalescence [1–3]. Foams and emulsions have a high specific surface area (i.e., are interface-dominated systems) and therefore their stability strongly depends on the protein's interfacial properties [4,5].

Surface activity (i.e., ability to increase surface pressure, or decrease interfacial tension) of the proteins is an important attribute in the droplet formation process but does not explain bubble and droplet stability over time. For this, dilatational rheological properties are relevant, as they directly affect the propensity of droplets to resist coalescence [2,6]. The interfacial properties of dairy proteins (i.e., caseins and whey proteins) have already been widely studied. The flexible caseins tend to adsorb rapidly at the interface but the resulting film elasticity is low due to the lack of intermolecular protein interactions [7–9]. In comparison, globular dairy proteins such as bovine serum albumin (BSA), lysozyme and β-lactoglobulin (β-lg) adsorb slower but form stronger viscoelastic films, which is attributed to their ability to form densely packed monolayers with in-plane protein-protein interactions at both the air- and oil-water interface [10,11].

Proteins from legume plants such as soy and pea are gaining interest as more sustainable protein sources, and the interfacial properties of their main constituents have also been investigated. For soy, that is glycinin and β-conglycinin [12–15]; and for pea, vicilin and legumin [16,17]. Soy proteins have been shown to adsorb slowly at the air- and oil-water interface due to their compact and large structure, as a result of hydrophobic intermolecular interactions [18]. Recent work also showed that the soluble fraction of soy or pea proteins forms interfacial layers with an elasticity close to that of whey protein-based films, at a stripped oil-water interface, but the layers were less interconnected and

* Corresponding author at: Laboratory of Food Process Engineering, Bornse Weilanden 9, 6708 WG Wageningen, the Netherlands.
E-mail address: emma.hinderink@wur.nl (E.B.A. Hinderink).

https://doi.org/10.1016/j.colsurfb.2020.111015
Received 21 February 2020; Received in revised form 1 April 2020; Accepted 3 April 2020
Available online 18 April 2020

less stretchable [19]. Yet, when used in emulsions, soluble pea proteins were outperformed by dairy proteins, i.e., the former lead to larger and less physically stable droplets [20].

Using blends of plant and dairy proteins might be the solution to strive for sustainability while not compromising technological functionality. In contrast to mixtures of proteins from the same biological origin (e.g., casein and whey protein), the interfacial behavior of plant-dairy proteins has been studied only scarcely. Blending soy or pea proteins with whey proteins or sodium caseinate led to interfacial elasticities at the stripped oil-water interface between those of the individual proteins, suggesting that both proteins contributed to the elasticity of the interfacial film [21]. However, the underlying film structure and protein interactions are not yet understood.

Interfacial behavior is often characterized with a Langmuir trough or an automated drop tensiometer [22] that both allow for surface pressure to be followed over time, as well as for interfacial dilatational rheology to be studied. A Langmuir trough can also be combined with ellipsometry to record film thickness [23,24], and to construct Langmuir-Blodgett (LB)-films of which the structural heterogeneity can be assessed by atomic force microscopy (AFM) [25]. The advantage of LB-films in combination with AFM is the length scale at which the interfaces are studied, typically the nanometer scale [10,26], which is relevant to the size of protein molecules and small supramolecular structures.

The range of available techniques to study the oil-water interface is more limited than for the air-water interface, and consequently, emulsifying properties are often related to air-water interface measurements. Protein adsorption and interfacial rheology have already been compared for air- and oil-water interfaces, leading to contradictory conclusions. Williams & Prins (1996) reported no difference in the elastic moduli for β-casein and β-lg at the oil- or air-water interface. Krägel et al. (2003) (for β-lg) and Santiago et al. (2008) (for soy proteins) found a faster increase of the surface pressure at the oil-water interface compared to the air-water interface, which they linked to facilitated protrusion of the hydrophobic parts of the protein into the oil phase. As a result, thicker adsorbed layers were formed compared to the air-water interface, onto which proteins spread more which led to thinner layers showing smaller changes in surface pressure [27]. The difference between data recorded at air- or oil-water interfaces is not surprising, when considering the fact that protein adsorption at the oil-water interface already varies for different oil types, with more polar oils inducing less protein unfolding, which results in lower surface pressures and slower interfacial network formation [28].

Herein, we aim to understand the protein-protein interactions at the interface, and the interactions of the proteins with the adjoining bulk phases to design well-defined plant-dairy protein films. We considered whey protein isolate (WPI) and sodium caseinate (SC) as dairy proteins, and the soluble fraction of pea protein isolate (PPI) as plant protein source. The individual proteins and their 1:1 (w/w) blends were extensively studied at the air-water interface (Langmuir trough, LB-films + AFM, ellipsometry, automated drop tensiometer) and at the stripped sunflower oil-water interface (automated drop tensiometer).

2. Experimental

2.1. Materials

WPI, purity 97.0–98.4 % (BiPro®, Davisco, Switzerland), SC, purity 97 % (Excellion™, Sodium Caseinate S, FrieslandCampina, the Netherlands), and PPI, 80–90 % purity (NUTRALYS s85 F, Roquette, France) were used as received. Sodium phosphate dibasic (Na_2HPO_4), sodium phosphate monobasic (NaH_2PO_4) were purchased from Sigma Aldric (Saint Louis, USA). The soluble protein concentration was determined using a bicinchoninic acid (BCA) kit (BCA1 − 1 KT, Sigma-Aldrich, Saint Louis, USA). Sunflower oil was purchased from a local supermarket and stripped with Florisil (Sigma-Aldrich, 20,281, Supelco, 100–200 mesh) to remove surface-active impurities, as described previously [29]. Ultrapure water was obtained from a Milli-Q system (Millipore Corporation, Billerica, Massachusetts, US) and used for all the experiments.

2.2. Preparation of aqueous phases

WPI and SC (1 wt.%) were dissolved in a 10 mM phosphate buffer (pH = 7.0) and stirred overnight at 4 °C. PPI was dispersed in the same buffer (6 wt.%) and stirred for at least 48 h at 4 °C. The insoluble part was removed by centrifugation (16,000 × g, 30 min), and the supernatant was re-centrifuged in similar conditions, after which the second supernatant was collected and used for the experiments. A BCA assay (Smith et al., 1985) was used to determine the protein content of the supernatant, as described previously [20]. The protein solutions were diluted to 1 g/L for air-water measurements, or 0.1 g/L for oil-water measurements.

2.3. Automated drop tensiometer measurements

The interfacial tension between air or stripped sunflower oil and the protein solutions in 10 mM phosphate buffer was measured with an automated drop tensiometer (Tracker, Teclis, Longessaigne, France). A pendant drop was used for the air-water measurements, a rising drop for the oil-water experiments (i.e., a drop of oil was immersed in a cuvette filled with the protein solution) using 20-gauge needles. SC, WPI, and PPI were tested individually as well as 1:1 (w/w) plant-dairy protein blends. The interfacial tension was recorded for 3.5 h at 20 °C, using a drop area of 15 mm^2 for the air-water experiments, and 30 mm^2 for the oil-water experiments. The interfacial tension was calculated based on the shape of the droplet using the Laplace equation [30].

After 3.5 h, amplitude sweeps were performed with a constant frequency of 0.1 Hz. The droplet interface was compressed and expanded in a sinusoidal way, ranging from 5 to 30 % deformation. In the frequency sweep experiments, the oscillation frequency was varied from 0.002 to 0.1 Hz, while the amplitude was kept constant (5 %). For both the amplitude and frequency sweeps, 5 deformation cycles were done, after which 5 rest cycles were applied before the next deformation started. The oscillating surface tension signal was analyzed with a Fast Fourier transform, and the intensity and phase of the first harmonic was used to calculate the dilatational elastic modulus (E_d') and the dilatational viscous modulus (E_d") according to Eq.s 1 and 2.

$$E'_d = \Delta\gamma\left(\frac{A_0}{\Delta A}\right)\cos\delta \quad (1)$$

$$E''_d = \Delta\gamma\left(\frac{A_0}{\Delta A}\right)\sin\delta \quad (2)$$

Here $\Delta\gamma$ is the difference in interfacial tension, A_0 the initial droplet/bubble area, ΔA the amplitude of change in area, and δ the phase shift of the oscillating interfacial tension signal, compared to the induced area change. This first harmonic-based analysis is accurate in the linear response regime. Outside this regime, higher harmonics are present that can be analyzed by Lissajous plots in which the change in surface pressure ($\pi = \gamma\text{-}\gamma_0$) is plotted against the oscillating deformation signal (30 %) [31].

2.4. Structural organization of interfacial films

Langmuir isotherms and Langmuir Blodgett films were made at the air-water interface using a KSV NIMA Langmuir trough (medium size, 364 × 76 mm, Biolin Scientific, Espoo, Finland). Buffer was used as substrate and 34 µL of 1 g/L protein solution were spread on the surface. The interfacial layer was equilibrated for 30 min before barriers were closed at a speed of 5 mm/min. Langmuir-Blodgett (LB) films were deposited on a freshly cleaved mica plate that was immersed into the

sub phase before the proteins were spread. The films were loaded at a surface pressure of 20 mN/m, with an upward speed of 1 mm/min. They were next dried in a desiccator at least overnight prior to analysis with an atomic force microscope (AFM; MultiMode 8-HRTM, Bruker, Billerica, US). Images were recorded in the tapping mode using non-conductive pyramidal silicon nitride probes with a nominal spring constant of 0.40 N/m (Bruker, Billerica, US). A lateral scan frequency of 0.977 Hz was used, and the resolution was set at 512 × 512 pixels in a scan area of $2 \times 2\,\mu m^2$. The AFM images were analyzed with NanoScope Analysis 1.5 software.

Film thickness at the air-water interface was measured using an imaging ellipsometer nanofilm EP4 (Accurion GmbH, Goettingen, Germany) in combination with a KSV NIMA Langmuir trough (size, 580 × 145 mm, Biolin Scientific, Espoo, Finland). The trough was filled with phosphate buffer (10 mM) and 200 µL of 1 g/L protein solution were spread on the surface. The interfacial layer was equilibrated for 30 min before barriers were closed at a speed of 5 mm/min until the desired surface pressure was reached. The ellipsometric angles Ψ and Δ were measured at different wavelengths using a filter wheel from 499.8 to 739.8 nm, and an exposure time of $1.5{\cdot}10^5$ ms. Buffer without proteins was measured five times and used to determine the refractive index, n and extinction coefficient, k, and a Cauchy distribution was used to calculate the film thickness.

2.5. Experimental design

All measurements were performed in at least independent duplicates. The LB-films were imaged at least at two locations per film.

3. Results and discussion

3.1. Air-water interface

3.1.1. Adsorption kinetics and surface activity

The change in air-water surface pressure for the individual proteins and protein blends was monitored in time using an automated drop tensiometer (Fig. 1A). The surface pressure first rapidly increased, followed by a phase of slower increase, and subsequently even slower increase, which has be linked to binding, unfolding and reorganization of proteins at the interface, respectively [32]. Clear differences were found between the individual proteins; at the end of the experiment, PPI-stabilized interfaces showed the highest surface pressure of 28.8 ± 0.8 mN/m, SC was at 25.9 ± 0.8 mN/m, and WPI was the lowest at 23.3 ± 1.3 mN/m. However, initially SC increased the surface pressure the fastest (Appendix, Fig. A1), followed by PPI and WPI. WPI consists of the globular proteins α-lactalbumin (α-La) and β-lactoglobulin (β-lg), whereas caseins have no secondary or tertiary structure and therefore adsorb and spread fast at the interface because less rearrangements occur [33]. Pea proteins adsorbed rapidly and increased the surface pressure the most over the measured time scale, which is probably related to their greater hydrophobicity compared to dairy proteins, imparting them with a higher driving force for adsorption [34]. The WPI-PPI blend-stabilized interface followed the surface pressure curve of the PPI-stabilized interface until a surface pressure of 29.0 ± 1.3, which could be indicative of a preferential adsorption of pea proteins. For the SC-PPI blend-stabilized interface, the surface pressure increased faster compared to PPI and SC alone, and (30.1 ± 0.8 mN/m) than SC only, indicating that protein adsorption seems to be accelerated and enhanced in the blend.

In the Langmuir trough, proteins were spread at the interface and subsequently compressed, which opposes the previously described experiments where film formation was driven by protein diffusion. The surface pressure isotherms differed for the individual proteins (Fig. 1B). Upon compression of the whey protein monolayer, the surface pressure first increased linearly (looking from right to left, i.e., while decreasing surface area), after which the increase levelled off, indicating that the adsorbed proteins interacted and changed conformation. In contrast, the pea protein film gave a linear response upon compression, indicating no specific interaction between proteins. For SC, the lowest surface pressure values were obtained; the surface pressure levelled off at 20 mN/m and only further increased to 21.7 ± 0.1 mN/m, which is close to the equilibrium spreading pressure of 22 mN/m for β-casein [35].

The isotherm for the WPI-PPI blend showed a lower increase in surface pressure compared to the one for WPI, but both were similar in shape, which suggests that whey proteins dominate the film behavior. The isotherm for SC-PPI first showed a linear increase in surface pressure, after which a plateau was reached at a surface pressure around 21 mN/m, followed by a second linear increase when compressing further, which makes this isotherm rather different from those of the individual constituent proteins. The plateau value was comparable to that of SC, which makes us believe that the surface pressure response of this blend was initially dominated by SC up to a value of 21 mN/m, after which the contribution of pea proteins became more prominent. At this stage, SC may be pushed out of the interface into the subphase, as was the case for the SC-stabilized interface, leading to surface domination by pea proteins.

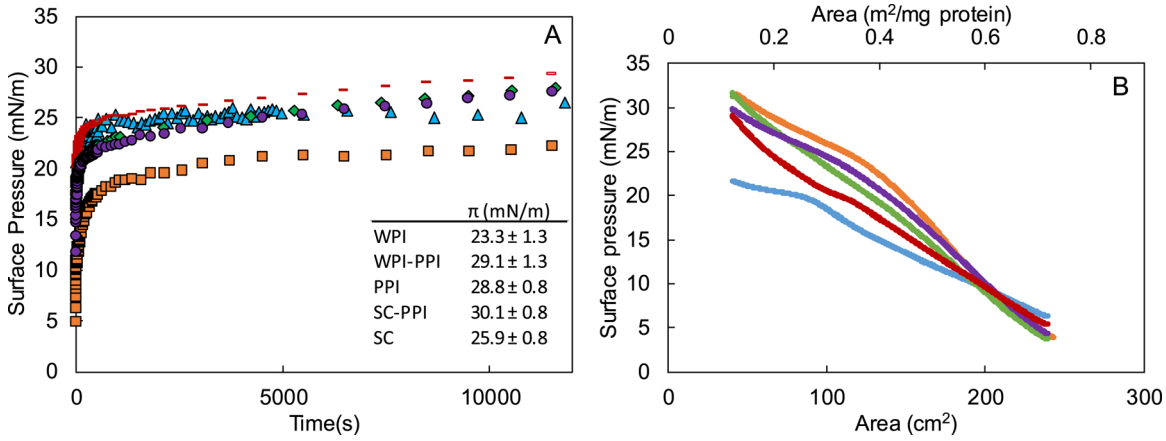

Fig. 1. A) Surface pressure using a pendant drop in an automated drop tensiometer at protein concentration 1 g/L at the air-water interface over time measured for WPI (■), SC (▲), PPI (◆) 1:1 SC-PPI (▬) and 1:1 WPI-PPI (●), the table reports the 'equilibrium' interfacial tension and B) Surface pressure isotherm of the individual proteins and their blends at the air-water interface measured by Langmuir trough for WPI (orange), SC (blue), PPI (green), 1:1 WPI-PPI (purple) and 1:1 SC-PPI (red). For clarity, one representative curve is shown per sample, but similar results were obtained on multiple independent replicates. (For interpretation of the references to colour in the Figure, the reader is referred to the web version of this article).

3.1.2. Interface structural organization

To further characterize the physical properties of the protein films involved in the surface pressure isotherm experiments, film thickness as a function of surface pressure was determined using an ellipsometer in combination with a Langmuir trough. At a surface pressure of 20 mN/m, SC formed the thickest layer (3.7 ± 0.15 nm), followed by SC-PPI (3.4 ± 0.28 nm), PPI (3.1 ± 0.14 nm), WPI-PPI (2.9 ± 0.07 nm) and WPI (2.1 ± 0.07). Compression of the interfacial layer led to an increase in film thickness, along with the previously described increase in surface pressure, for all systems tested. For SC, even though the surface pressure levelled off from a certain compression level, the film thickness may have increased due to molecules stacking below the primary monolayer [35], albeit rather loosely due to the disordered structure of the caseins. Interestingly, the SC-PPI-stabilized interface was able to reach a surface pressure of 26 mN/m and was thicker (5.5 ± 0.71 nm) compared to the PPI-based layer (4.8 ± 0.64 nm). This suggests that when present in this blend, SC remains at the interface together with the pea proteins, which is also confirmed by the high surface pressures reported in Fig. 1A, and linked to faster increase of the surface pressure, which has been related to thicker interfacial layers [27,36].

It should be pointed out that ellipsometer data reflect an average film thickness; when looking at the LB films constructed at 20 mN/m (Figs. 2 and 3) it is clear that all films are structurally heterogenous. In these LB films, a noticeable difference occurs between WPI, PPI or WPI-PPI (both globular proteins) and SC or SC-PPI (containing disordered SC); films containing SC show some large clusters, whereas in all other films the clusters are smaller. At low surface pressures, caseins spread at the interface (< 20 mN/m) but upon compression loops are formed in the aqueous phase [37]. The large clusters in the SC-containing LB films may thus correspond to protein material protruding into the aqueous phase as induced by the compression process. Structural heterogeneity is common in protein films, as found for e.g., β-lg [38], β-casein [39] and WPI [40] and oxidative modified PPI [41].

3.1.3. Interface rheological properties

Oscillatory dilatational amplitude sweeps (sinusoidal deformation 5–30 %) at a frequency of 0.01 Hz were performed after an adsorption and equilibration time of 3.5 h. Elastic (E_d') and viscous (E_d") moduli were calculated from the oscillatory data and plotted as function of the applied deformation amplitude. For all proteins tested, elastic moduli (Fig. 4A) were substantially higher than viscous moduli (Appendix, Fig. A2).

The elastic moduli of the WPI-stabilized air-water interface decreased from 56 mN/m at 5% deformation to 21 mN/m at 30 % deformation (Fig. 4A). This strain dependence of the elastic modulus indicates that the interfacial network weakened upon deformation, which can be attributed to the ability of β-lactoglobulin to form disulphide linkages in a highly interconnected network, that weakens upon deformation [42]. The strain dependence was less for WPI-PPI- (E_d' only varied from 25 to 20 mN/m) and not present in PPI-, SC-, and SC-PPI-stabilized interfaces. The elastic moduli of the SC-stabilized interface were below 10 mN/m, which made them the weakest among all proteins tested. This can be explained by the fact that casein monolayers are loosely packed with weak protein-protein interactions [7]. However, when SC was combined with PPI, the values for E_d' were similar to those recorded for interfaces with PPI only, which implies that either PPI dominates the SC-PPI-stabilized interface, or interactions occur between the PPI and SC, leading to a response similar to that of PPI. For WPI-PPI-stabilized interfaces, the elastic moduli are in between those of WPI- and PPI-based layers, suggesting the presence of both proteins at the interface.

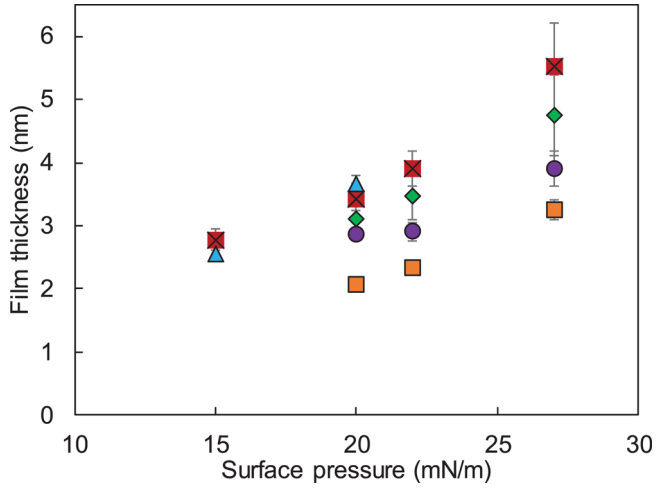

Fig. 2. Film thickness for WPI (■), SC (▲), PPI (◆) 1:1 SC-PPI (✖) and 1:1 WPI-PPI (●) at the air-water interface as function of the surface pressure. Error bars represent the standard deviation of multiple measurements on at least two independent replicates.

Oscillatory dilatational frequency sweeps (0.002 − 0.05 Hz) were performed at fixed amplitude of 5%. Again, elastic moduli were higher than viscous moduli, and only the elastic moduli are reported as function of frequency, on a double logarithmic scale (Fig. 4B). WPI formed the most elastic layer (highest E_d') followed by WPI-PPI, SC-PPI and PPI, whereas SC formed the layer with the lowest E_d', which is in line with the amplitude sweep results. The slope of the double logarithmic plot of elastic moduli as function of frequency was around 0.1, which is typical for soft glassy interfaces, and implies that the contribution of diffusional exchange of protein between the bulk and the interface to the response is negligible [43].

To understand these effects in a more detailed way, Lissajous plots were used, that show the surface pressure as a function of the deformation during oscillatory dilatational experiments, and thus provide information about the interfacial network behavior in extension and compression. The advantage of Lissajous plots is that nonlinear effects are not neglected, and they thus give a richer impression of surface behavior, as compared to simply calculating moduli. In brief, a linear shape of the Lissajous plot indicates a purely elastic behavior, and a spherical shape a viscous behavior of the interface. Linear viscoelastic responses result in an ellipse-shaped plot, and non-linear behavior leads to asymmetric shapes [31], as shown in Fig. 5 top left. All systems tested gave predominantly elastic responses upon 30 % deformation i.e., $\Delta A/A_0 = 0.3$ (Fig. 5) but also showed asymmetries that are indicative of a nonlinear response, even when the apparent modulus appeared to be strain independent. This clearly indicates the benefit of Lissajous plots over the first harmonics approach.

SC, PPI, and SC-PPI-stabilized interfaces gave a nonlinear viscoelastic response, dominated by elasticity (narrow ellipse). At the start of extension (the lower left corner of the plot, at $\Delta A/A_0 =$ -0.3) the surface pressure first increased, after which it levelled off towards maximum extension ($\Delta A/A_0 =$ +0.3). This is a signature of interfacial strain softening in extension, due to disruption of the interfacial microstructure. Upon compression the reverse phenomenon happened, which indicates strain stiffening due to increased surface density of clustered protein regions, approaching a jammed state [22]. This strain softening in extension and strain hardening upon compression is typical for protein-stabilized interfaces. For the SC-stabilized interface, lower surface pressures compared to PPI- and SC-PPI-stabilized interfaces were found at maximum extension, but similar surface pressures at maximum compression. We reported earlier a thicker interfacial layer (Fig. 2), and higher surface pressure (Fig. 1A) for the SC-PPI blend compared to its individual counterparts. Combining this with the Lissajous plot results allows us to conclude that enhanced protein adsorption in this specific blend has led to the improved dilatational elasticity compared to SC only, that does however not surpass that of PPI only.

WPI-stabilized interfaces are more viscous than the others (also seen

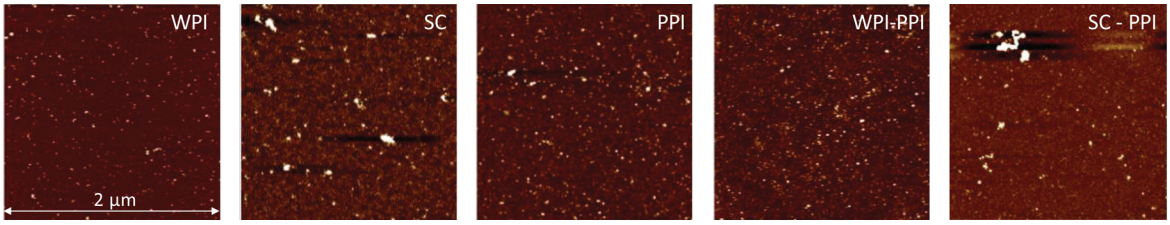

Fig. 3. AFM images of LB films prepared with the individual proteins (WPI, SC, PPI) and their blends. LB films are constructed at the air-water interface at a surface pressure of 20 mN/m, and imaged after drying at room temperature. The overall layer height is up to 5.3 nm, with black representing the lowest areas and white the highest ones. For clarity, one representative image is shown per sample, but similar results were obtained on multiple independent replicates.

in the loss moduli in Appendix, Fig. A2), and the plot is relatively wide at the lower left part as a result of yielding of the surface microstructure upon the start of the extension. It is clear from the apparent moduli reported in Fig. 4A that the WPI-stabilized interfaces are the stiffest (due to stronger in-plane protein-protein interactions). When a certain surface stress is exceeded the microstructure yields, and starts to flow towards maximum extension when the slope approaches almost zero, indicating a predominantly viscous response. The shape of the Lissajous plot is typical for WPI-stabilized air-water interfaces as recently reported by [40]. The interface based on the WPI-PPI blend showed a more elastic response compared to PPI alone, with strain softening in extension and strain stiffening in compression, and a less viscous behavior compared to WPI. The plot suggests that both proteins were present at the interface, which could not be that clearly concluded from Fig. 1A.

To conclude, blending PPI with SC gave a synergistic behavior at the air-water interface, in the sense that PPI helped retaining SC at the interface upon compression, and increased the interfacial elasticity compared to SC alone. In contrast blending PPI with WPI hindered the formation of an interconnected network, typical for WPI-stabilized interfaces.

3.2. Oil-water interface

3.2.1. Adsorption kinetics and interfacial activity

At the oil-water interface, layers made of pure PPI or SC led to the highest surface pressure (~18 mN/m), and WPI to the lowest (~17 mN/m) (Fig. 6), with SC increasing surface pressure the fastest (Fig. 6A). The curve corresponding to the WPI-PPI-stabilized interface was initially between those of the WPI- and PPI-stabilized interfaces, and towards the end of the measurement, closer to that of pure WPI. The curve corresponding to the SC-PPI-stabilized interface was in between those of the SC and PPI-stabilized interfaces, but eventually a similar pseudo-equilibrium surface pressure was reached for PPI, SC and SC-PPI-stabilized interfaces. For all protein systems tested, the surface pressure increased less at the oil-water interface than at the air-water interface (Fig. 1A). Please keep in mind that oil-water interface experiments were performed at 0.1 g/L protein solution whereas for the air-water it was 1 g/L, which implies that the local protein concentration in the immediate vicinity of the interface differed by one order of magnitude.

3.2.2. Interface rheological properties

At the oil-water interface, the apparent elastic moduli of the WPI-, PPI- and WPI-PPI-stabilized layers decreased upon deformation (Fig. 7). This strain dependence was the strongest for the WPI-based layer, which showed a decrease from 32 to 18 mN/m, and the lowest for PPI and WPI-PPI (i.e., decrease from 20 to 16 mN/m for both). The SC-PPI- and SC-stabilized interfaces were the weakest with elastic moduli of 8.5 and 4.5 mN/m, respectively, and no strain dependence, indicating weaker in-plane protein interactions for these systems. The elastic moduli of all interfaces were lower at the oil-water interface compared to the air-water interface (Fig. 4) except for the PPI-stabilized interface, which had an elastic modulus of 15 mN/m and no strain-dependence at the air-water interface. Remarkably, the WPI-PPI-stabilized layers exhibited the same moduli as the PPI-stabilized ones, which was not the case at the air-water interface, and indicates that either only pea proteins adsorbed, or the structure and interactions within the film are

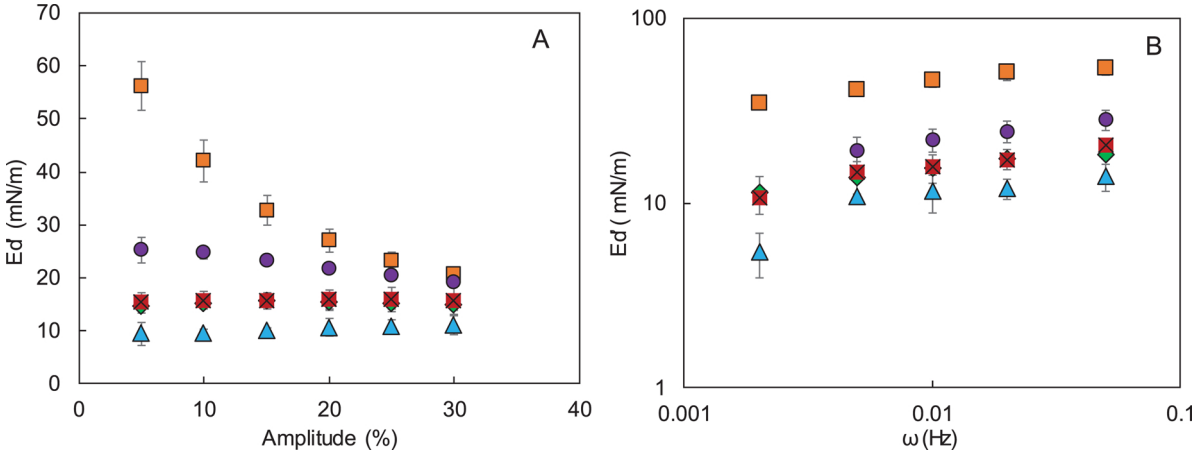

Fig. 4. Apparent dilatational elastic moduli (Ed') at the air-water interfaces stabilized by WPI (■), SC (▲), PPI (◆) 1:1 SC-PPI (✖), and 1:1 WPI-PPI (●) blend A) as a function the applied deformation (frequency, 0.01 Hz) and B) as a function of the applied frequency (amplitude, 5%). Error bars represent the standard deviation of multiple measurements on at least two independent replicates.

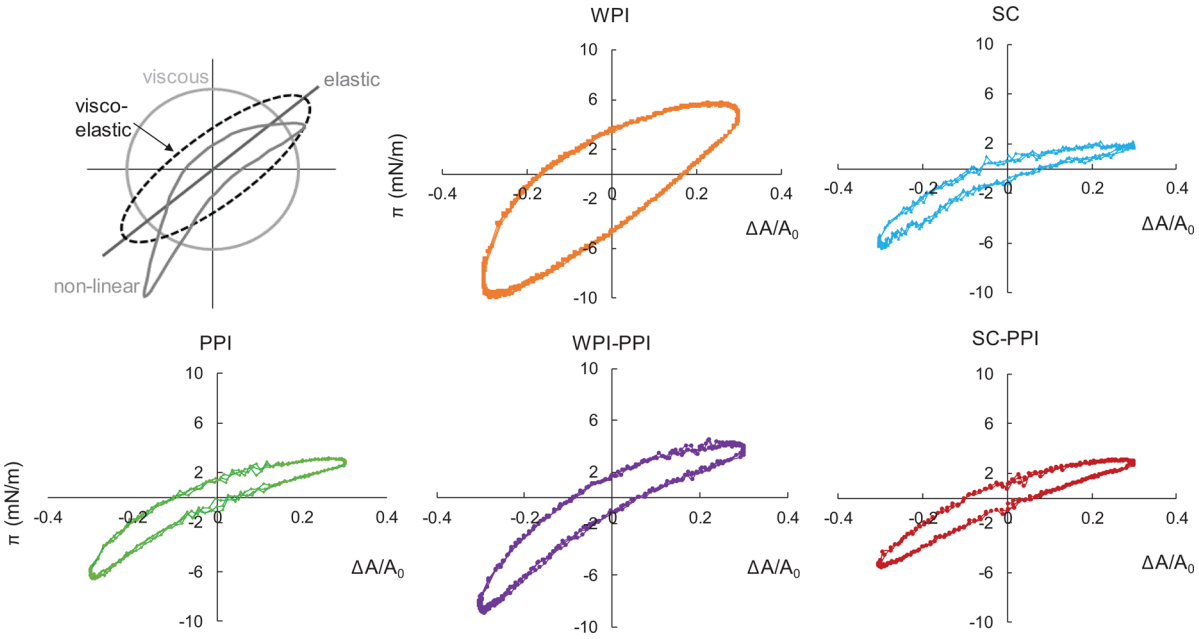

Fig. 5. Example of Lissajous plots depicting viscous, elastic, viscoelastic and non-linear viscoelastic interfaces in top left; and Lissajous plots at 30 % dilatational deformation and oscillation frequency at 0.01 Hz at the air-water interface for WPI (orange), SC (blue), PPI (green), 1:1 WPI-PPI (purple) and 1:1 SC-PPI (red). For clarity only one replicate is shown, but similar results were obtained for at least independent duplicates. (For interpretation of the references to colour in the Figure, the reader is referred to the web version of this article).

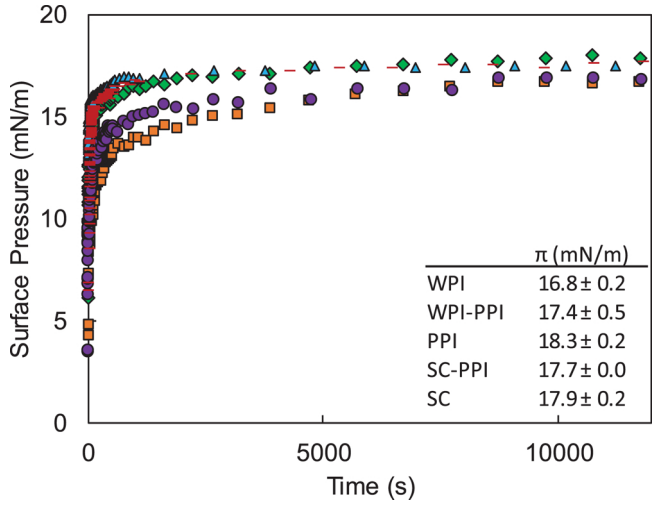

Fig. 6. Surface pressure over 3.5 h (the insert table gives pseudo-equilibrium interfacial tension, i.e., the average of the last 20 points) for whey protein (WPI,■), sodium caseinate (SC,▲), pea protein (PPI, ◆), 1:1 whey protein-pea protein blend (WPI-PPI, ●) and 1:1 sodium caseinate-pea protein blend (SC-PPI,▬) at the stripped sunflower oil-water interface. For clarity, one representative curve is shown per sample, but similar results were obtained on multiple independent replicates.

similar with the blend or PPI alone.

Oscillatory dilatational frequency sweeps (0.002 − 0.05 Hz) were performed at a fixed amplitude of 5 %, and the elastic moduli were plotted as function of applied frequency on a double logarithmic scale (Fig. 7B). Whey proteins formed the most elastic layer (highest E_d'), followed by WPI-PPI and PPI, SC-PPI, and SC as the lowest, which is in line with the amplitude sweep results. For WPI-, PPI- and WPI-PPI-stabilized interfaces a slope close to 0.1 was found, which implies that the contribution of diffusion from the bulk to the interface was negligible, as explained earlier [43]. For the SC- and SC-PPI-stabilized interfaces, the slope was 0.25, indicating that diffusion-controlled processes may have contributed to the response to deformations, which is different from the findings at the air-water interface. It was reported that β-casein increased the surface pressure faster at the oil-water interface compared to the air-water interface, which was related to the possibility of the protein to penetrate into the oil phase with its longer hydrophobic chain, leaving only a short hydrophilic tail interacting with the water phase [44].

The surface pressure as a function of the deformation (amplitude equal to 30 %) was plotted in Lissajous plots for all systems tested (Fig. 8), and showed strain softening in extension and strain hardening upon compression, with clear differences between the interfaces. The WPI-stabilized interface was predominantly elastic, as seen from the narrow shape of the plot, and the Lissajous plot was similar to previous ones reported in literature [45,46]. For the PPI-stabilized interface, the lower left part of the graph has a pointy shape, which means that upon compression and subsequent extension a similar response in surface pressure was measured, indicative of weak in-plane attractive interactions. When such interactions are strong, the densification induced by the compression can lead to a significant increase in the stiffness of the structure, which then results in a steep slope of the Lissajous plot upon extension of the interface (compare to WPI at the air-water interface, which shows strong protein-protein interaction, in Fig. 5). The Lissajous plot of the WPI-PPI-stabilized interface showed the same response upon deformation, which may be interpreted as PPI dominating the interface, although that is not that likely since the surface pressure of WPI-PPI is very close to that of WPI (Fig. 6B). Most likely, both proteins are at the interface, with pea proteins hindering whey protein network formation, resulting in a less interconnected and less elastic interface compared to whey protein-based layer with dilatational properties similar to those found for PPI only.

The SC-stabilized oil-water interface gave an almost linear viscoelastic response with almost no strain softening nor hardening in extension and compression. This, together with the relatively high exponent found in the frequency dependence, indicates that the in-plane interactions are too weak to induce network formation, and that the response is dominated by exchange of SC between bulk and interface.

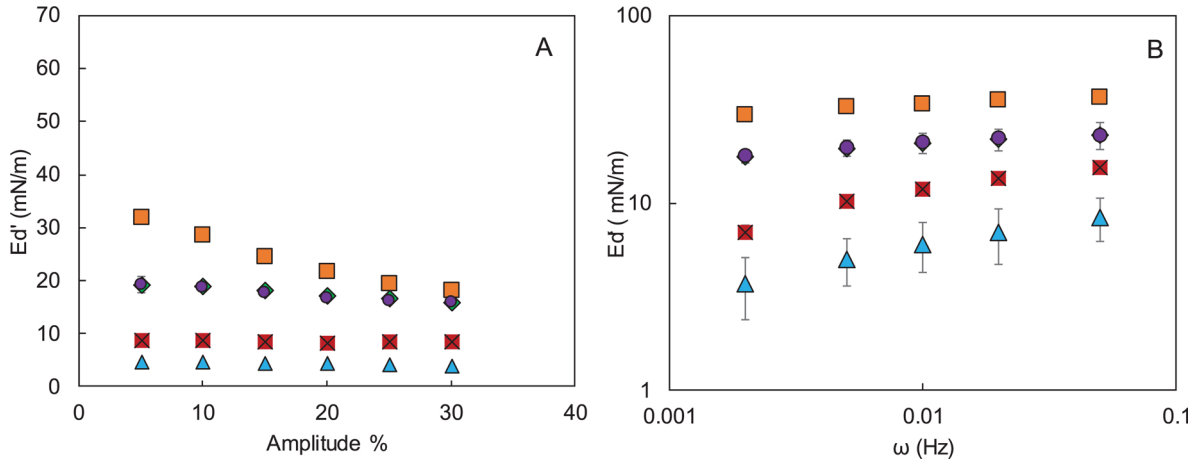

Fig. 7. Apparent dilatational elastic moduli (E_d') at the oil-water interfaces stabilized by WPI (■), SC (▲), PPI (◆) 1:1 SC-PPI (■) and 1:1 WPI-PPI (●) blend A) as a function the applied deformation (frequency, 0.01 Hz) and B) as a function of the applied frequency (amplitude, 5%). Error bars represent the standard deviation of multiple measurements on at least two independent replicates.

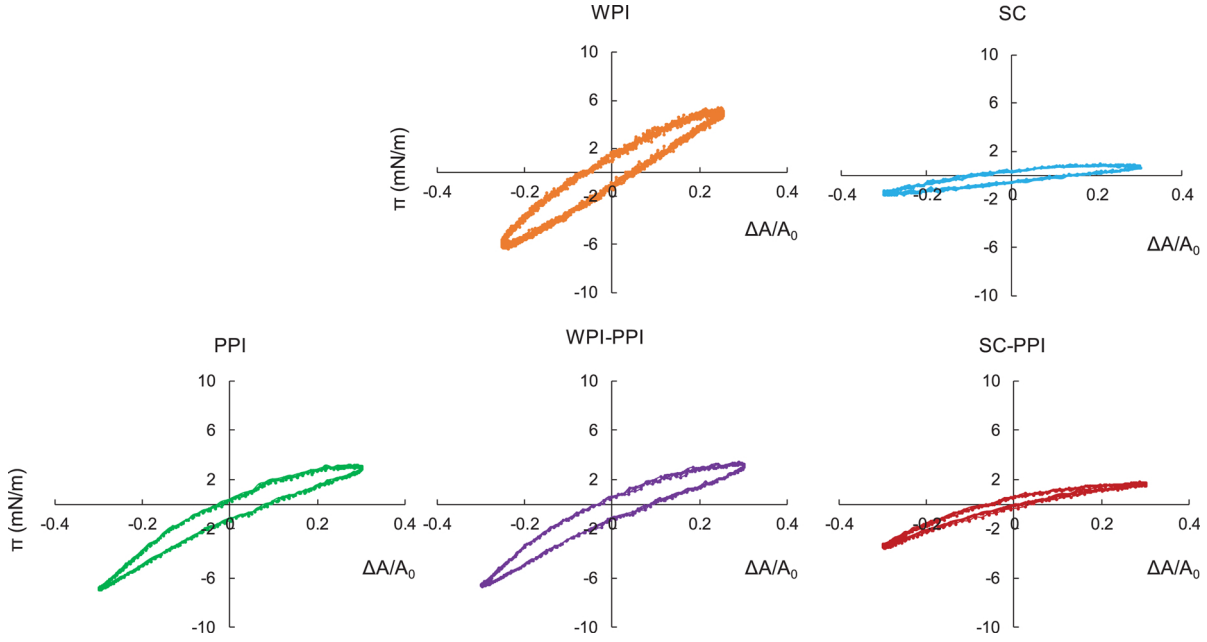

Fig. 8. Lissajous plots at 30 % dilatational deformation and oscillation frequency at 0.01 Hz at the oil-water interface for WPI (orange), SC (blue), PPI (green), 1:1 WPI-PPI (purple) and 1:1 SC-PPI (red). For clarity only one replicate is shown, but similar results were obtained for at least independent duplicates. (For interpretation of the references to colour in the Figure, the reader is referred to the web version of this article).

For the SC-PPI-stabilized interface, an extremely narrow plot was obtained, for which the slope levels off in extension, and increases in compression. As observed for the air-water interface, in-plane network formation did not occur, and the surface concentration of the proteins merely increases upon compression and decreases upon extension. The resulting changes in the surface tension led to a plot resembling a curved line.

3.3. Our results put in a wider perspective

In literature, various effects have been described regarding protein adsorption and network formation at the oil- or air-water interfaces, and here we summarize them and use them to put into perspective the results that are reported herein. In general, it is assumed that globular proteins unfold at the interface with the oil-phase acting as a solvent for the hydrophobic segments, which reduces the van der Waals cohesion between the apolar side chains of the proteins [35]. This also implies that globular proteins can unfold more at the oil-water compared to the air-water interface [47–49]. In the present study, elastic moduli were higher, except for PPI-stabilized interfaces, at the air-water interface, which may be explained by hydrophobic intra-protein interactions that are hindered by solvation in the oil phase [48]. Furthermore, it has been suggested that the solvent quality affects interfacial viscoelastic moduli. Benjamins et al. (2006) compared the interfacial elastic modulus of ovalbumin and β-lactoglobulin adsorbed at triacylglycerol-, hydrocarbon- or air-water interfaces, and found that triacylglycerol was the best solvent and air the worst. He found a strong correlation between the interfacial tension of the bare interface and interfacial elastic moduli [50]. It has to be noted that in that respect, an oil phase is not always a better solvent phase compared to air; higher elastic moduli of β-lg were found at the *n*-tetradecane interface compared to the air-water interface [51], and we also found that PPI gave higher moduli at

the oil-water interface.

It has been suggested that the polarity of the oil is a good indication for the extent of protein unfolding, with more polar oils leading to less protein unfolding and less surface pressure changes [28]. Next to the decrease of hydrophobic interactions by solvation in the oil phase, there are also differences in the in-plane electrostatic repulsion between proteins for the two interfaces. The dielectric constant of air is approximately 1 [50], and that of sunflower oil about 3 [52]. That means that the electrostatic repulsion between the proteins (which has the nature of a dipole-dipole interaction because of the asymmetry in the counter-ion distribution) is shorter-ranged for the oil-water interface. This would result in increased attractive protein interactions, possibly leading to a higher modulus if this effect is larger than the reduction of attractive interactions due to improved solvent quality.

It is clear that in the tested blends, PPI hinders the formation of elastic WPI-layers at both interfaces, whereas it improved the elasticity of the SC-stabilized interface at both interfaces. When blending WPI with soy protein isolate (SPI), that by itself produces interfaces with lower moduli than WPI, this leads to interfaces that closely resemble those of pure WPI [21]. This suggests that the interactions between SPI and WPI are stronger compared to those between WPI and PPI reported herein, and that such interactions are highly protein- and blend-specific.

4. Conclusions

We investigated the interfacial properties of dairy proteins (WPI, SC), plant protein (PPI) and their 1:1 blends (WPI-PPI, SC-PPI) at the air- and oil-water interfaces (Appendix, Fig. A3). At the air-water interface, WPI formed the thinnest layer that consists of an interconnected network with superior stiffness compared to all the other systems tested. Blending WPI with PPI decreased the layer elasticity compared to WPI alone, but gave a stronger layer compared to PPI alone. SC formed the weakest interfacial layer, and blending it with PPI improved the layer's mechanical strength. The SC-PPI interfacial layer had the same strength as the PPI-stabilized interface, and PPI was able to retain SC at the interface, therewith forming thicker layers compared to layers made of the individual counterparts. At the oil-water interface, PPI and WPI-PPI had a similar behavior when subjected to dilatational deformation, and formed weaker layers compared to WPI. Blending SC with PPI gave stronger interfacial layers compared to SC alone, but the layers were inferior in stiffness compared to the layers formed with WPI, PPI and WPI-PPI.

Overall, lower elastic moduli were found at the oil-water interface compared to the air-water interface, due to the ability of the oil phase to interact with the hydrophobic parts of the proteins, therewith acting as a solvent. This solvation hindered the inter-protein hydrophobic interactions and, as a result, interfacial layers with lower connectivity were formed, which led to lower elastic moduli. We concluded that the interfacial properties of individual proteins are not additive and highly depend on the interface used, which should be considered when attempting to explain the performance of food dispersions based on the involved interfacial properties..

CRediT authorship contribution statement

Emma B.A. Hinderink: Conceptualization, Data curation, Formal analysis, Methodology, Visualization, Writing - original draft. **Leonard Sagis:** Methodology, Formal analysis, Supervision, Writing - review & editing. **Karin Schroën:** Supervision, Writing - review & editing. **Claire C. Berton-Carabin:** Visualization, Methodology, Formal analysis, Supervision, Writing - review & editing.

Declaration of Competing Interest

None.

Acknowledgments

The project is organized by and executed under the auspices of TiFN, a public - private partnership on precompetitive research in food and nutrition. The authors have declared that no competing interests exist in the writing of this publication. Funding for this research was obtained from Fromageries Bel S.A., Nutricia Research B.V., Pepsico Inc., Unilever R&D Vlaardingen B.V., the Netherlands Organisation for Scientific Research and the Top-sector Agri&Food. The authors wish to thank Regina Giovani for performing preliminary experiments.

Appendix A

Fig. A3

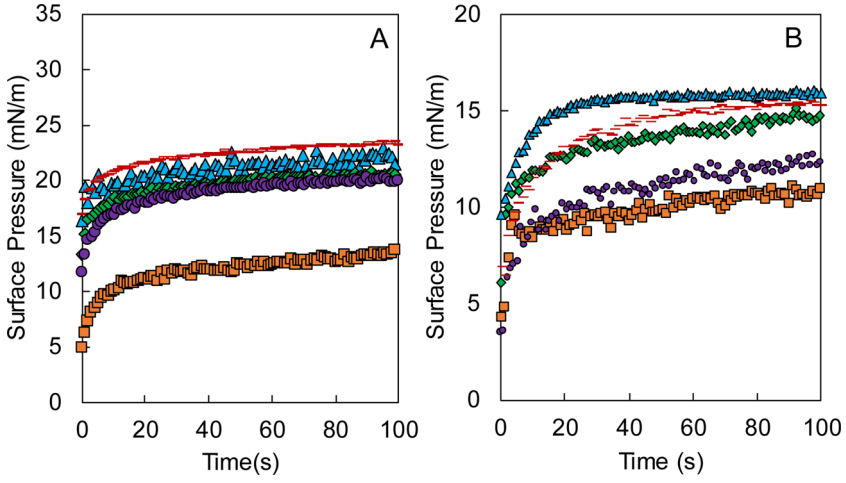

Fig. A1. A) Surface pressure using a pendant drop in the automated drop tensiometer of 1 g/L protein B) surface pressure using a rising drop in the automated drop tensiometer at 0.1 g/L protein in the first 100 s of protein adsorption.

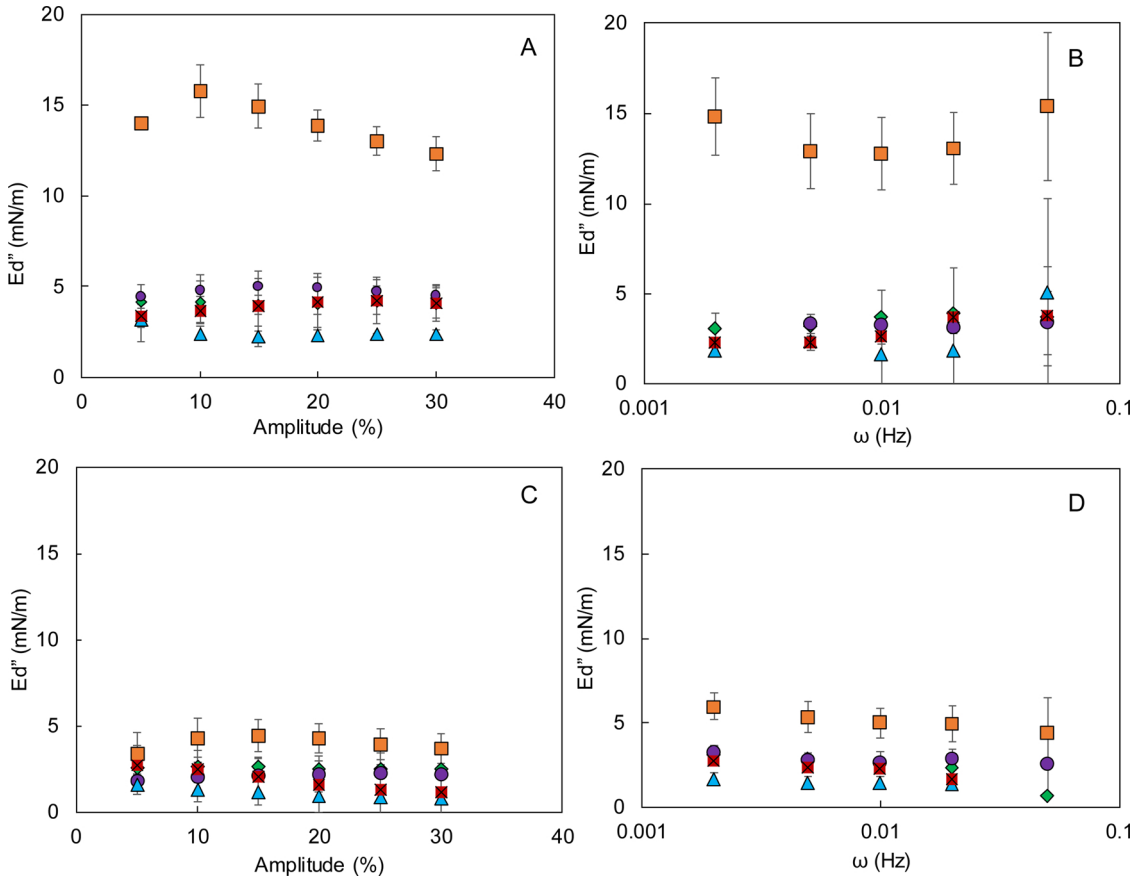

Fig. A2. Dilatational loss moduli (E_d') of interfaces stabilized by WPI (■), SC (▲), PPI (◆) 1:1 SC-PPI (■) and 1:1 WPI-PPI (●) blend as A-C) a function the applied deformation (frequency, 0.01 Hz) and B-D) a function of the applied frequency (amplitude, 5%) at the air-water (A,B) or oil-water interface (C,D). Error bars represent the standard deviation of at least two independent replicates.

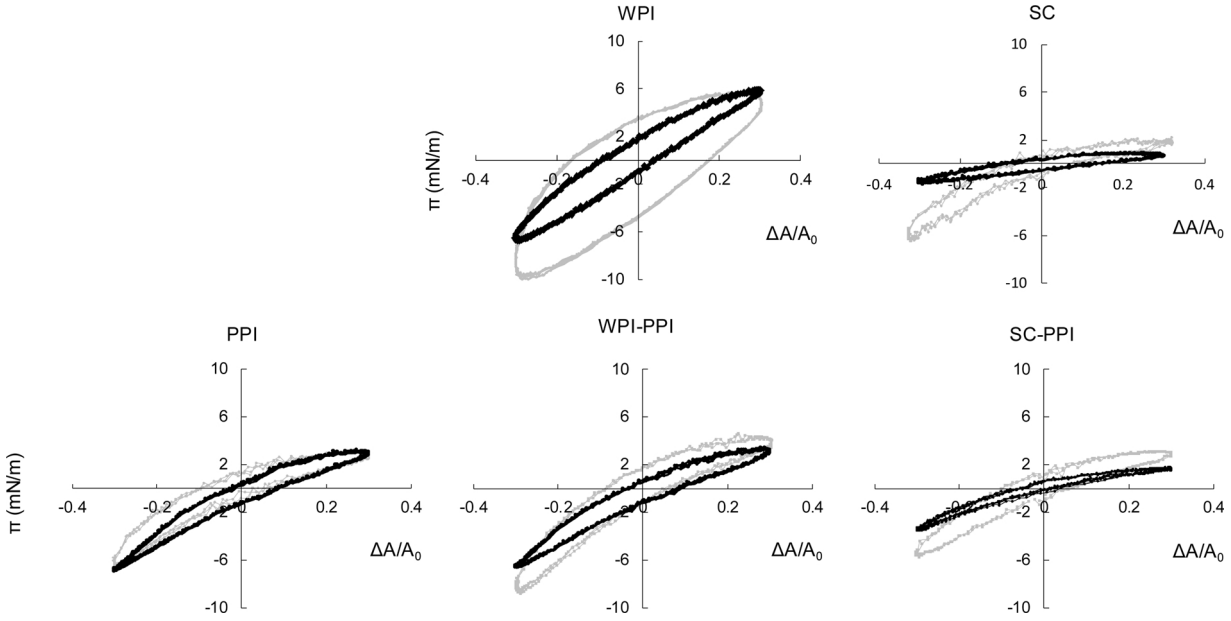

Fig. A3. Lissajous plots at the air-water interface (grey) and oil-water interface (black) at 30 % deformation.

References

[1] D.J. McClements, Protein-stabilized emulsions, Curr. Opin. Colloid Interface Sci. 9 (2004) 305–313, https://doi.org/10.1016/j.cocis.2004.09.003.
[2] M.A. Bos, T. Van Vliet, Interfacial rheological properties of adsorbed protein layers and surfactants: a review, Adv. Colloid Interface Sci. 91 (2001) 437–471, https://doi.org/10.1016/S0001-8686(00)00077-4.
[3] E. Dickinson, Adsorbed protein layers at fluid interfaces: interactions, structure and surface rheology, Colloids Surf. B Biointerfaces 15 (1999) 161–176, https://doi.org/10.1016/S0927-7765(99)00042-9.
[4] C.C. Berton-Carabin, L. Sagis, K. Schroën, Formation, structure, and functionality of

interfacial layers in food emulsions, Annu. Rev. Food Sci. Technol. 9 (2018) 551–587, https://doi.org/10.1146/annurev-food-030117-012405.
[5] L.M.C. Sagis, Dynamic properties of interfaces in soft matter: experiments and theory, Rev. Mod. Phys. 83 (2011) 1367–1403, https://doi.org/10.1103/RevModPhys.83.1367.
[6] B.S. Murray, Rheological properties of protein films, Curr. Opin. Colloid Interface Sci. 16 (2011) 27–35, https://doi.org/10.1016/j.cocis.2010.06.005.
[7] E. Dickinson, Milk protein interfacial layers and the relationship to emulsion stability and rheology, Colloids Surf. B Biointerfaces 20 (2001) 197–210, https://doi.org/10.1016/S0927-7765(00)00204-6.
[8] D.E. Graham, M.C. Phillips, Proteins at liquid interfaces II adsorption isotherms, J. Colloid Interface Sci. 70 (1979).
[9] D.E. Graham, M.C. Phillips, Proteins at liquid interfaces IV. dilatational properties, J. Colloid Interface Sci. 76 (1980).
[10] E. Dickinson, Mixed biopolymers at interfaces: competitive adsorption and multilayer structures, Food Hydrocoll. 25 (2011) 1966–1983, https://doi.org/10.1016/j.foodhyd.2010.12.001.
[11] A. Williams, A. Prins, Comparison of the dilational behaviour of adsorbed milk proteins in the air-water and oil-water interfaces, Colloids Surfaces A Physicochem. Eng. Asph. 114 (1996) 267–275, https://doi.org/10.1016/0927-7757(96)03534-0.
[12] V.P. Ruíz-Henestrosa, C.C. Sánchez, Mdel M.Y. Escobar, J.J.P. Jiménez, F.M. Rodríguez, J.M.R. Patino, Interfacial and foaming characteristics of soy globulins as a function of pH and ionic strength, Colloids Surfaces A Physicochem. Eng. Asph. 309 (2007) 202–215, https://doi.org/10.1016/j.colsurfa.2007.01.030.
[13] A.H. Martin, M.B.J. Meinders, M.A. Bos, M.A. Cohen Stuart, T. Van Vliet, Conformational aspects of proteins at the air/water interface studied by infrared reflection-absorption spectroscopy, Langmuir. 19 (2003) 2922–2928, https://doi.org/10.1021/la0208629.
[14] J.R. Wagner, J. Guéguen, Surface functional properties of native, acid-treated, and reduced soy glycinin. 2. Emulsifying properties, J. Agric. Food Chem. 47 (1999) 2181–2187, https://doi.org/10.1021/jf9809784.
[15] M. Keerati-u-rai, M. Miriani, S. Iametti, F. Bonomi, M. Corredig, Structural changes of soy proteins at the oil-water interface studied by fluorescence spectroscopy, Colloids Surf. B Biointerfaces 93 (2012) 41–48, https://doi.org/10.1016/j.colsurfb.2011.12.002.
[16] C. Dagorn-Scavinier, J. Gueguen, J. Lefebvre, A comparison of interfacial behaviours of pea (Pisum sativum L.) legumin and vicilin at air/water interface, Food / Nahrung. 30 (1986) 337–347, https://doi.org/10.1002/food.19860300332.
[17] C. Dagorn-Scavinier, J. Gueguen, J. Lefebvre, Emulsifying properties of pea globulins as related to their adsorption behaviors, J. Food Sci. 52 (1987) 335–341, https://doi.org/10.1111/j.1365-2621.1987.tb06607.x.
[18] L.G. Santiago, J. Maldonado-Valderrama, A. Martín-Molina, C. Haro-Pérez, J. García-Martínez, A. Martín-Rodríguez, M.A. Cabrerizo-Vílchez, M.J. Gálvez-Ruiz, Adsorption of soy protein isolate at air-water and oil-water interfaces, Colloids Surfaces A Physicochem. Eng. Asp. 323 (2008) 155–162, https://doi.org/10.1016/j.colsurfa.2007.11.001.
[19] K.K.H.Y. Ho, K. Schroën, M.F.S. Martín-González, C.C. Berton-Carabin, Physicochemical stability of lycopene-loaded emulsions stabilized by plant or dairy proteins, Food Struct. 12 (2017) 34–42, https://doi.org/10.1016/j.foostr.2016.12.001.
[20] E.B.A. Hinderink, K. Münch, L. Sagis, K. Schroën, C.C. Berton-Carabin, Synergistic stabilisation of emulsions by blends of dairy and soluble pea proteins: contribution of the interfacial composition, Food Hydrocoll. 97 (2019), https://doi.org/10.1016/j.foodhyd.2019.105206.
[21] K.K.H.Y. Ho, K. Schroën, F.M. Martín-González, C.C. Berton-Carabin, Synergistic and antagonistic effects of plant and dairy protein blends on the physicochemical stability of lycopene-loaded emulsions, Food Hydrocoll. 81 (2018) 180–190, https://doi.org/10.1016/j.foodhyd.2018.02.033.
[22] L.M.C. Sagis, P. Fischer, Nonlinear rheology of complex fluid-fluid interfaces, Curr. Opin. Colloid Interface Sci. 19 (2014) 520–529, https://doi.org/10.1016/j.cocis.2014.09.003.
[23] D.E. Graham, M.C. Phillips, Proteins at liquid interfaces, J. Colloid Interface Sci. 70 (1979) 427–439, https://doi.org/10.1016/0021-9797(79)90050-X.
[24] P. Wilde, A. Mackie, F. Husband, P. Gunning, V. Morris, Proteins and emulsifiers at liquid interfaces, Adv. Colloid Interface Sci. 108–109 (2004) 63–71, https://doi.org/10.1016/j.cis.2003.10.011.
[25] L.M.C. Sagis, B. Liu, Y. Li, J. Essers, J. Yang, A. Moghimikheirabadi, E. Hinderink, C. Berton-Carabin, K. Schroen, Dynamic heterogeneity in complex interfaces of soft interface-dominated materials, Sci. Rep. 9 (2019) 2938, https://doi.org/10.1038/s41598-019-39761-7.
[26] C. Bernardini, S.D. Stoyanov, L.N. Arnaudov, M.A. Cohen Stuart, Colloids in Flatland: a perspective on 2D phase-separated systems, characterisation methods, and lineactant design, Chem. Soc. Rev. 42 (2013) 2100–2129, https://doi.org/10.1039/c2cs35269a.
[27] J. Krägel, M. O'Neill, A.V. Makievski, M. Michel, M.E. Leser, R. Miller, Dynamics of mixed protein-surfactant layers adsorbed at the water/air and water/oil interface, Colloids Surf. B Biointerfaces 31 (2003) 107–114, https://doi.org/10.1016/S0927-7765(03)00047-X.
[28] J. Bergfreund, P. Bertsch, S. Kuster, P. Fischer, Effect of oil hydrophobicity on the adsorption and rheology of β-Lactoglobulin at oil-water interfaces, Langmuir. 34 (2018) 4929–4936, https://doi.org/10.1021/acs.langmuir.8b00458.
[29] C. Berton, C. Genot, M.H. Ropers, Quantification of unadsorbed protein and surfactant emulsifiers in oil-in-water emulsions, J. Colloid Interface Sci. 354 (2011) 739–748, https://doi.org/10.1016/j.jcis.2010.11.055.
[30] J. Benjamins, A. Cagna, E.H. Lucassen-Reynders, Viscoelastic properties of triacylglycerol/water interfaces covered by proteins, Colloids Surfaces A Physicochem. Eng. Asp. 114 (1996) 245–254, https://doi.org/10.1016/0927-7757(96)03533-9.
[31] L.M.C. Sagis, E. Scholten, Complex interfaces in food: structure and mechanical properties, Trends Food Sci. Technol. 37 (2014) 59–71, https://doi.org/10.1016/j.tifs.2014.02.009.
[32] C.J. Beverung, C.J. Radke, H.W. Blanch, Protein adsorption at the oil/water interface: characterization of adsorption kinetics by dynamic interfacial tension measurements, Biophys. Chem. 81 (1999) 59–80 http://www.ncbi.nlm.nih.gov/pubmed/10520251.
[33] J. Maldonado-valderrama, V.B. Fainerman, M. Jose, M.A. Cabrerizo-vı, R. Miller, Dilatational Rheology of -Casein Adsorbed Layers at Liquid - Fluid Interfaces, (2005), pp. 17608–17616.
[34] P.A. Wierenga, M.B.J. Meinders, M.R. Egmond, F.A.G.J. Voragen, H.H.J. De Jongh, Protein exposed hydrophobicity reduces the kinetic barrier for adsorption of Ovalbumin to the air-water interface, Langmuir. 19 (2003) 8964–8970, https://doi.org/10.1021/la034868p.
[35] D.E. Graham, M.C. Phillips, Proteins at liquid interfaces III molecular structures, J. Colloid Interface Sci. 70 (1979).
[36] J. Benjamins, Static and Dynamic Properties of Proteins Adsorbed at Liquid Interfaces, (2000).
[37] F. MacRitchie, Reversibility of protein adsorption, Stud. Interface Sci. 7 (1998) 149–177, https://doi.org/10.1016/S1383-7303(98)80051-3.
[38] P.A. Rühs, C. Affolter, E.J. Windhab, P. Fischer, Shear and dilatational linear and nonlinear subphase controlled interfacial rheology of β-lactoglobulin fibrils and their derivatives, J. Rheol. (N. Y. N. Y). 57 (2013) 1003–1022, https://doi.org/10.1122/1.4802051.
[39] C. Berton-Carabin, C. Genot, C. Gaillard, D. Guibert, M.H. Ropers, Design of interfacial films to control lipid oxidation in oil-in-water emulsions, Food Hydrocoll. 33 (2013) 99–105, https://doi.org/10.1016/j.foodhyd.2013.02.021.
[40] J. Yang, I. Thielen, C.C. Berton-Carabin, E. van der Linden, L.M.C. Sagis, Nonlinear interfacial rheology and atomic force microscopy of air-water interfaces stabilized by whey protein beads and their constituents, Food Hydrocoll. 101 (2020) 105466, , https://doi.org/10.1016/j.foodhyd.2019.105466.
[41] E.B.A. Hinderink, W. Kaade, L. Sagis, K. Schroën, C.C. Berton-carabin, Microfluidic investigation of the coalescence susceptibility of pea protein-stabilised emulsions: effect of protein oxidation level, Food Hydrocoll. 102 (2020), https://doi.org/10.1016/j.foodhyd.2019.105610.
[42] E. Dickinson, S.E. Rolfe, D.G. Dalgleish, Surface shear viscometry as a probe of protein-protein interactions in mixed milk protein films adsorbed at the oil-water interface, Int. J. Biol. Macromol. 12 (1990) 189–194, https://doi.org/10.1016/0141-8130(90)90031-5.
[43] S.E.H.J. van Kempen, H.A. Schols, E. van der Linden, L.M.C. Sagis, Non-linear surface dilatational rheology as a tool for understanding microstructures of air/water interfaces stabilized by oligofructose fatty acid esters, Soft Matter 9 (2013) 9579, https://doi.org/10.1039/c3sm51770e.
[44] C. Kotsmar, E.V. Aksenenko, V.B. Fainerman, V. Pradines, J. Krägel, R. Miller, Equilibrium and dynamics of adsorption of mixed β-casein/surfactant solutions at the water/hexane interface, Colloids Surfaces A Physicochem. Eng. Asp. 354 (2010) 210–217, https://doi.org/10.1016/j.colsurfa.2009.04.025.
[45] C.C. Berton-Carabin, A. Schröder, A. Rovalino-Cordova, K. Schroën, L. Sagis, Protein and lipid oxidation affect the viscoelasticity of whey protein layers at the oil-water interface, Eur. J. Lipid Sci. Technol. 118 (2016) 1630–1643, https://doi.org/10.1002/ejlt.201600066.
[46] K.K.H.Y. Ho, K. Schroën, F.M. Martín-González, C.C. Berton-Carabin, Synergistic and antagonistic effects of plant and dairy protein blends on the physicochemical stability of lycopene-loaded emulsions, Food Hydrocoll. 81 (2018) 180–190, https://doi.org/10.1016/j.foodhyd.2018.02.033.
[47] B.S. Murray, P.V. Nelson, A novel langmuir trough for equilibrium and dynamic measurements on air – Water and oil – Water monolayers, Langmuir 12 (1996) 5973–5976, https://doi.org/10.1021/la960748o.
[48] R. Wüstneck, B. Moser, G. Muschiolik, Interfacial dilational behaviour of adsorbed β-lactoglobulin layers at the different fluid interfaces, Colloids Surf. B Biointerfaces 15 (1999) 263–273, https://doi.org/10.1016/S0927-7765(99)00093-4.
[49] V. Mitropoulos, A. Mütze, P. Fischer, Mechanical properties of protein adsorption layers at the air / water and oil / water interface: A comparison in light of the thermodynamical stability of proteins, Adv. Colloid Interface Sci. 206 (2014) 195–206, https://doi.org/10.1016/j.cis.2013.11.004.
[50] J. Benjamins, J. Lyklema, E.H. Lucassen-Reynders, Compression/expansion rheology of oil/water interfaces with adsorbed proteins, Comparison with the air/water surface, Langmuir. 22 (2006) 6181–6188, https://doi.org/10.1021/la060441h.
[51] B.S. Murray, A. Ventura, C. Lallemant, Dilatational rheology of protein-non-ionic surfactant films at air-water and oil-water interfaces, Colloids Surfaces A Physicochem. Eng. Asp. 143 (1998) 211–219, https://doi.org/10.1016/S0927-7757(98)00256-8.
[52] T. Prevc, B. Cigić, R. Vidrih, N. Poklar Ulrih, N. Šegatin, Correlation of basic oil quality indices and electrical properties of model vegetable oil systems, J. Agric. Food Chem. 61 (2013) 11355–11362, https://doi.org/10.1021/jf402943b.